Hemodynamic Safety Assurance in Closed-Loop Controlled Critical Care: Hemorrhage Resuscitation and Sedation Case Study

Weidi Yin, Ali Tivay, Hosam K. Fathy, and Jin-Oh Hahn, Senior Member, IEEE

Abstract—This letter presents a novel approach to assure hemodynamic safety in closed-loop controlled critical care. The approach is equipped with safetypreserving control based on control barrier functions to ensure the safety of hemodynamic state, hemodynamic monitoring to estimate hemodynamic state, probabilistic recursive therapeutic target guidance to direct a patient as closely as possible to a prescribed therapeutic target along a desired trajectory. A notable advantage of the approach is that it can be augmented to single-input-single-output critical care control loops developed in isolation to guard hemodynamic safety against conflicts between them, providing a practical alternative to sophisticated multi-input-multi-output control loop design. The efficacy of the approach was examined in a hemorrhage resuscitation-intravenous sedation case study using realistic virtual patients. The approach as a whole assured the boundedness of hemodynamic state by reconciling conflicts between the two control loops. The recursive therapeutic target guidance directed patients to personalized reachable targets while maintaining the patients' therapeutic responses near the desired therapeutic trajectory. The approach may serve as an effective means to reconcile multiple critical care control loops and assure holistic hemodynamic safety.

Index Terms—Control barrier function, virtual patient, hemorrhage, sedation, recursive guidance.

I. INTRODUCTION

HERE is a bursting interest in closed-loop control of critical care treatments including fluid resuscitation [1], vasopressor therapy [2], [3], anesthesia and analgesia [4], [5], and mechanical ventilation [6], [7] to name a few, by virtue of its ability to devote to patient care with full vigilance. In fact, recent reports have suggested clinical feasibility of closed-loop control in individual treatments [8]–[10].

However, the state-of-the-art is not yet mature enough to be reliably deployed to real-world critical care settings in which multiple treatments are administered concurrently to a patient.

This work was supported in part by the U.S. Office of Naval Research (N00014-19-1-2402) and the U.S. National Science Foundation (CMMI-1760817 and CNS-1748762). (Corresponding author: J.-O. Hahn).

W. Yin, A. Tivay, H.K. Fathy, and J.O. Hahn are with the Department of Mechanical Engineering, University of Maryland, College Park, MD 20742, USA (e-mail: wyin12@umd.edu, tivay@umd.edu, hfathy@umd.edu, and hhahn12@umd.edu).

Existing critical care controllers are designed for individual treatments on a loop-by-loop basis, with little considerations for inter-loop interferences. When multiple treatments are to be administered to a patient, closed-loop controllers developed in isolation are stacked in tandem with practically no account for potential conflicts between them and their ultimate impact on patient safety [11]–[14], other than ad-hoc restrictions on therapeutic targets [4] and means [9] as well as their manual adjustments by clinicians [12]. A natural alternative is multi-input multi-output control design. But, it may be inefficient and even intractable to design provably safe high-dimensional controllers suited to a large number of heterogeneous critical care treatments. Hence, a practical solution may be to develop an add-on capability that can be augmented to mediate already existing single-input single-output critical care controllers.

This work intends to develop a novel practically deployable approach to reconcile conflicts between multiple closed-loop controlled critical care treatments and assure patient safety. Our approach consists of safety-preserving control based on control barrier functions (CBFs) [15] to mediate individually developed single-input-single-output critical care controllers, hemodynamic monitoring to estimate state variables required to realize the safety-preserving control, and probabilistic recursive therapeutic target guidance to direct a patient to a prescribed therapeutic target as closely as possible along a desired path. We use hemorrhage resuscitation-intravenous (IV) propofol sedation as a case study, which is relevant in that these treatments can exhibit conflicting interactions and compromise hemodynamic safety: hemorrhage resuscitation to achieve a blood pressure (BP) target dilutes propofol in the blood and weakens its intended effect, while propofol interrupts hemorrhage resuscitation by inducing vasodilation and venodilation that lowers BP. Hence, although closed-loop controlled treatments appear to successfully direct a patient to prescribed BP and sedation targets, the internal hemodynamics of the patient, represented by cardiac output (CO) and total peripheral resistance (TPR), can often be pushed to an unacceptably dangerous state [16].

II. MATHEMATICAL MODEL AND VIRTUAL PATIENTS

A. Mathematical Model

We employed a mathematical model capable of replicating the combined hemodynamic effects of hemorrhage resuscitation and IV sedation developed and validated in our prior work [16]. The mathematical model is equipped with (i) blood volume (BV) kinetics in arteries and veins including vessel-tissue fluid exchange, (ii) homeostatic compensatory control of CO, TPR, and unstressed BV to maintain BP, and (iii) pharmacology of the IV sedative propofol. The BV kinetics represents the changes in arterial and venous BV and BP in response to fluid resuscitation:

$$\dot{V}_A(t) = Q(t) - [P_A(t) - P_V(t)]/R(t) - J_E(t) \tag{1}$$

$$\dot{V}_V(t) = -Q(t) + [P_A(t) - P_V(t)]/R(t) + J_R(t)$$
 (2)

where V_A and V_V are arterial and venous BV (including plasma and red blood cell (RBC) volumes), Q is CO, R is TPR, P_A and P_V are arterial and venous BP, and J_R and J_E are the rates of fluid gain and vessel-tissue fluid exchange. P_A and P_V relate to V_A and V_V by vessel capacitances:

$$P_A(t) - P_{A0} = (V_A(t) - V_{A0})/C_A$$
 (3)

$$P_V(t) - P_{V0} = (V_V(t) - V_{V0} - (V_{VU}(t) - V_{VU0}))/C_V$$
 (4)

where P_{A0} and P_{V0} are nominal arterial and venous BP, V_{VU} is unstressed venous BV, V_{A0} , V_{V0} , V_{VU0} are nominal arterial, venous, and unstressed venous BV, and C_A and C_V are arterial and venous capacitances. Total BV, V, is given by the sum of V_A and V_V :

$$V(t) = V_A(t) + V_V(t) \tag{5}$$

The vessel-tissue fluid exchange is modeled to replicate the capillary filtration and lymphatic flow following the change in BV in such a way that the resuscitated fluid is ultimately distributed into BV and the fluid volume in the tissues per a prescribed fraction. Denoting r_B the prescribed change in BV

in the steady state in response to
$$J_R$$
:

$$r_B(t) = \frac{1}{1+\alpha_R} \int_0^t J_R(\tau) d\tau \tag{6}$$

where α_R is the ratio between the changes in BV and tissue fluid volume in the steady state due to resuscitated fluid, the vessel-tissue fluid exchange is modeled as a proportional compensation to let $V(t) - V_0$ converge to $r_B(t)$:

$$J_{E}(t) = K_{E}(V(t) - V_{0} - r_{B}(t))$$
(7)

where V_0 is nominal BV, and K_E is a gain constant.

The homeostatic compensatory control to maintain BP is phenomenologically modeled in such a way that (i) CO compensates for the change in venous BP, (ii) TPR and unstressed venous BV compensate for the change in arterial BP, and (iii) TPR decreases as blood viscosity decreases:

$$\dot{s}_Q(t) = -p_C s_Q(t) + (z_C - p_C) \Delta P_V(t)$$

$$\Delta Q(t) = K_C s_Q(t) + K_C \Delta P_V(t) \tag{8}$$

$$\dot{s}_R(t) + p_R s_R(t) = -\Delta P_A(t)$$

$$\Delta R(t) = K_R s_R(t) + K_H \Delta H(t) - G_R C_e(t)$$
(9)

$$\Delta V_{VU}(t) = K_{VU}S_R(t) + G_{VU}C_e(t)$$
(10)

where $\Delta Q(t) = Q(t) - Q_0$, $\Delta R(t) = R(t) - R_0$, $\Delta P_A(t) =$ $P_A(t) - P_{A0}$, $\Delta P_V(t) = P_V(t) - P_{V0}$ with Q_0 and R_0 being nominal CO and TPR, $\Delta H(t) = H(t) - H_0$ where H(t) is blood hematocrit defined as $H(t) = \frac{V_{RBC}}{V_A(t) + V_V(t)}$ (where V_{RBC} is

red blood cell volume) and H_0 is its nominal value, K_C , K_R , K_H , and K_{VU} are gains, p_C and z_C are pole and zero related to the CO dynamics, p_R is pole related to the vasomotor tone dynamics, and G_R and G_{VU} are gains related to vasodilation and venodilation effects of propofol.

The propofol pharmacology is modeled as a compartmental drug mixing model (11)-(13), a 1st-order effect site delay model (14), and drug effect models (9)-(10) and (15) [17]:

$$\dot{m}_1(t) = -(k_{10} + k_{12} + k_{13})m_1(t) + k_{21}m_2(t) +$$

$$k_{31}m_3(t) + J_P(t) \tag{11}$$

$$m_2(t) = k_{12}m_1(t) - k_{21}m_2(t)$$
 (12)

$$\dot{m}_3(t) = k_{13}m_1(t) - k_{31}m_3(t) \tag{13}$$

$$\dot{C}_{e}(t) = -k_{e0}C_{e}(t) + \frac{V_{P}k_{e0}m_{1}(t)}{V_{D}(V_{A}(t) + V_{V}(t) - V_{RBC})}$$
(14)

$$BIS(t) = F_{RIS}(C_e(t)) \tag{15}$$

where m_1 , m_2 , and m_3 are propofol mass in the central as well as fast and slow peripheral compartments, k_{10} , k_{12} , k_{13} , k_{21} , and k_{31} are rate constants, J_P is propofol administration rate, C_e is effect site propofol concentration, k_{e0} is effect site time constant, V_D and V_P are nominal central distribution and plasma volumes, and $F_{BIS}(\cdot)$ is a sigmoidal function relating C_{ρ} to BIS, a widely used sedation measure [18].

B. Virtual Patient Generation

We derived a virtual patient (VP) generator pertaining to the mathematical model in II.A by applying it and datasets acquired in prior works [19], [20] to a collective variational inference (C-VI) method developed by us [21]. In brief, the C-VI method represents the hierarchical relationship between a cohort of patients and each individual patient therein into a probabilistic graphical model (PGM). The PGM embodies the notion that the set of model parameter values pertaining to each patient can be viewed as a sample taken from the cohortlevel model parameter distributions (which can be viewed as a VP generator), which encode typical behaviors anticipated from most patients in the cohort. For this PGM, the C-VI method infers the latent parameters specifying the probability density functions of both cohort-level and patient-specific parameter values in the mathematical model using modern variational inference techniques [22], [23] and stochastic optimization algorithms [24], [25]. In this work, we used the C-VI method to infer the means and standard deviations (SDs) of the probability density functions for all the parameters in the mathematical model both at cohort and individual subject levels. Then, we employed the cohort-level model parameter distributions as the VP generator for the mathematical model in II.A (via random sampling), both in the development (i.e., in specifying process noise for the development of a hemodynamic monitoring algorithm in III.B as well as in constructing a probabilistic reachability contour map as a basis for a probabilistic recursive therapeutic target guidance algorithm in III.C) and in silico evaluation (see IV) of the proposed approach.

III. HEMODYNAMIC SAFETY ASSURANCE APPROACH

Denoting $x \triangleq \{x_1, \dots, x_{10}\}$, where $x_1 = \Delta V_A$, $x_2 = \Delta V_V$, $x_3 = \Delta V_{VU}$, $x_4 = s_Q = \frac{1}{K_C} \Delta Q - \Delta P_V$, $x_5 = \Delta R$, $x_6 = r_B$, $x_7 = \frac{1}{K_C} \Delta Q - \frac{1}{K_C} \Delta Q -$ ΔC_e , $x_8 = \Delta m_1$, $x_9 = \Delta m_2$, and $x_{10} = \Delta m_3$, where all the deviations (i.e., Δs in x) are defined with respect to an initial state (when the algorithm is recruited), we reformulated the mathematical model in II.A as follows:

$$\dot{x}(t) = f(x) + g(x) \cdot u(t)$$

$$y(t_k) = h(x(t_k)) = \begin{bmatrix} P_A(t_k) \\ BIS(t_k) \end{bmatrix} = \begin{bmatrix} x_1(t_k)/C_A + P_{A0} \\ BIS(t_k) \end{bmatrix}$$
(16)

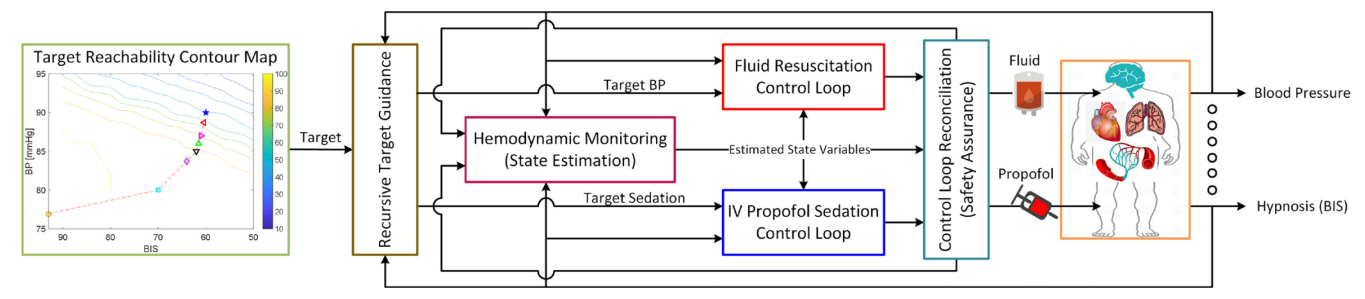


Fig. 1. Hemodynamic safety assurance based on probabilistic reachability-based recursive therapeutic target guidance, hemodynamic monitoring, and safety-preserving control loop reconciliation via control barrier functions.

where f(x) and g(x) are vector functions that can be derived from (1)-(15), $u(t) = [J_R \ J_P]^T$, and t_k is a sampling time instant. The control objective is to direct BP and BIS of a patient as closely as possible to a prescribed target while ensuring the boundedness of CO and TPR in a safe regime:

$$\min_{t \in \mathbb{R}} \lim_{t \to \infty} D(y(t), y_d(t)) \text{ s.t. } Q \le \overline{Q} \text{ and } R \ge \underline{R}$$
 (17)

where $D(y(t), y_d(t))$ is the distance between y(t) and $y_d(t)$ along a prescribed therapeutic trajectory, and \bar{O} and R are the upper bound of CO and the lower bound of TPR, respectively.

The proposed approach to accomplish the control objective is equipped with 3 main elements: safety-preserving control based on CBFs to ensure boundedness of CO and TPR, hemodynamic monitoring to estimate state variables required to realize the CBF-based control, and probabilistic reachability-based recursive therapeutic target guidance (Fig. 1). These elements, when combined, reconcile therapeutic goal and hemodynamic safety by enforcing the boundedness of hemodynamic variables (by CBFs) and directing a patient to a personalized reachable therapeutic target along a desired therapeutic trajectory with intermediate targets (by recursive target updates).

A. Safety Assurance via Control Barrier Functions

To preserve hemodynamic safety during closed-loop controlled hemorrhage resuscitation and IV sedation, we adopted a real-time optimization-based control strategy in which resuscitation inputs computed by the isolated closedloop hemorrhage resuscitation and IV sedation controllers are mediated by way of CBFs to ensure the forward invariance of hemodynamic variables in an admissible regime. context of hemorrhage resuscitation and IV propofol sedation, hemodynamic safety requires the upper-boundedness of CO and lower-boundedness of TPR to avoid over-resuscitation and subsequent vasodilation/venodilation. We expressed the boundedness constraints for CO and TPR as follows from (8)

$$h_1(x) = -Q_0 - K_C \left[x_4(t) + \frac{x_2(t) - x_3(t)}{c_V} \right] + \bar{Q} \ge 0$$
 (18)

$$h_2(x) = R_0 + x_5(t) - R \ge 0 \tag{19}$$

These constraints have relative degrees 1 and 2 with respect to J_R and J_P , respectively, which makes it impossible to mediate J_R and J_P concurrently using CBFs. Hence, we increased the relative degree pertaining to J_R by designing the actuator

dynamics and augmenting it to (6) as follows:
$$\epsilon \dot{x}_{11}(t) = -x_{11}(t) + J_R(t), \ r_B(t) = \frac{1}{1+\alpha_R} \int_0^t x_{11}(\tau) d\tau \quad (20)$$

where $\epsilon > 0$. Using (16) and (18)-(20), we constructed the following reciprocal CBF (R-CBF) candidates:

$$B_i(x) = \frac{1}{h_i(x)} + \operatorname{atan}\left(L_f \frac{1}{h_i(x)}\right) + \frac{\pi}{2}, \ i = 1,2$$
 (21)

Note that
$$\frac{1}{h_i(x)} \le B_i(x) \le \frac{1}{h_i(x)} + \pi$$
 and $L_g B_i(x) \ne 0$, $i = 1,2$.

Hence, it is possible to find u which satisfies the following inequalities for all x satisfying $h_i(x) > 0$, i = 1,2:

$$\inf_{x} \left[L_f B_i(x) + L_g B_i(x) \cdot u - \alpha (h_i(x)) \right] \le 0, \ i = 1,2$$
 (22)

where $\alpha(\cdot)$ is a class K function. Based on the R-CBFs (21), we formulated the following real-time quadratic programming (QP) problem to assure hemodynamic safety while guiding patients to a desired therapeutic target:

$$u^* = \arg\min_{u} \eta_1 \|J_R - \check{J}_R\|^2 + \eta_2 \|J_P - \check{J}_P\|^2$$
s.t. $\inf_{u} [L_f B_i(x) + L_g B_i(x) \cdot u - \alpha(h_i(x))] \le 0, i = 1,2$

$$J_R \ge 0, J_P \ge 0$$
(23)

where J_R and J_P are resuscitation inputs computed by the isolated fluid resuscitation and propofol sedation controllers (i.e., "Fluid Resuscitation Control Loop" and "IV Propofol Sedation Control Loop" in Fig. 1).

B. Hemodynamic Monitoring via Extended Kalman Filter

To realize the real-time QP-based control in (23) requires access to all the state variables. In this work, we employed an extended Kalman filter (EKF) based on the mathematical model in II.A developed in our prior work [26], which can estimate x(t) in real time from u(t) as well as BP and BIS measurements. For the design of the EKF, we defined the process noise and its covariance matrix to represent the effect of parametric uncertainty as derived in the VP generator [27], while we defined the sensor noise and its covariance matrix based on the noise variance associated with P_A and BIS. We then derived the state estimate \hat{x} using the EKF's recursive prediction and update procedure. The state \hat{x} thus estimated was used to solve the QP in (23).

C. Probabilistic Recursive Therapeutic Target Guidance

Hemorrhage resuscitation and IV sedation exert conflicting hemodynamic effects to each other. Hence, patients receiving these treatments concurrently may fail to reach a prescribed therapeutic target without violating hemodynamic safety. In addition, while preserving the boundedness of CO and TPR, the R-CBF-based mediation of resuscitation inputs in (22) can cause unpredictable drift in the therapeutic endpoints (i.e., BP and BIS), especially if the prescribed target is not reachable. To resolve these issues, we conceived a recursive target

TABLE I

DISTRIBUTIONS OF BP AND BIS ERRORS AS WELL AS MAXIMUM CO AND MINIMUM TPR VALUES IN HEMODYNAMICALLY (A) SAFE VS (B) UNSAFE VIRTUAL PATIENTS, IN THE ABSENCE AND PRESENCE OF THE PROPOSED APPROACH FOR RECONCILIATION OF HEMORRHAGE RESUSCITATION-IV PROPOFOL SEDATION CONTROL LOOPS.

(a) Hemodynamically safe virtual patients.

		BP Error [mmHg]	BIS Error [·]	Max CO [lpm]	Min TPR [mmHg/lpm]
	No Reconciliation	0 (-0~0)	0 (-0.2~0.1)	5.7+/-0.7	14.4+/-1.9
	Reconciliation	0 (-1~0)	0 (-0.1~0.1)	5.5+/-0.7	14.9+/-1.8

(b) Hemodynamically unsafe virtual patients.

	BP Error [mmHg]	BIS Error [·]	Max CO [lpm]	Min TPR [mmHg/lpm]
No Reconciliation	0 (-0~0)	0 (0.2~0.1)	8.5+/-1.3	9.4+/-1.6
Reconciliation	-5 (-6~-2)	1.3 (0.0~2.0)	6.3+/-1.2	11.9+/-2.2

guidance method based on probabilistic reachability. Its basic idea is to assess the probabilistic reachability of a prescribed therapeutic target, create a trajectory connecting the patient's current state to the prescribed therapeutic target and equip it with multiple intermediate targets with gradually decreasing probabilistic reachability, and direct a patient through these intermediate targets, in a sequential manner, as closely as possible to the prescribed therapeutic target while assuring that hemodynamic safety is preserved (Fig. 2).

In this work, we constructed a probabilistic reachability contour map in the BP-BIS plane numerically by simulating a large number of VPs with isolated single-input single-output hemorrhage resuscitation and IV sedation controllers. probabilistic reachability of a BP-BIS point was calculated as the percentage of the simulated VPs which reached the point without violating the inequalities (18)-(19). In this way, each BP-BIS point was assigned a probabilistic reachability value (meaning the possibility of taking the patient from an initial BP-BIS state to the point while maintaining hemodynamic safety). Then, we derived the desired therapeutic trajectory as the steepest descent path connecting the initial BP-BIS state and a prescribed BP-BIS therapeutic target, which is the shortest path in the sense of probabilistic reachability. On the trajectory, we introduced intermediate therapeutic targets in 5% probability increment from the therapeutic target. During the closed-loop controlled treatment, the approach initially presents the easiest (i.e., closest to the initial state; e.g., cyan square in Fig. 2) intermediate BP-BIS target to the isolated closed-loop controllers to compute \check{J}_R and \check{J}_P , which is then mediated by the QP (23) to derive J_R and J_P administered to the patient. If the presented intermediate target is reached (determined by BP error < 0.3 mmHg and BIS error < 0.1), it sequentially presents increasingly challenging intermediate targets to the closed-loop controllers. However, it reverts to the previous target if hemodynamic safety is violated (i.e., if \check{J}_R and \check{J}_P computed by the isolated single-input single-output closed-loop controllers violate the inequality in (22)), at which point it stops updating the therapeutic target.

IV. In SILICO EVALUATION

To evaluate the efficacy of the proposed approach, we created and used 100 VPs using the VP generator derived in II.B. In addition, we designed and used two single-input-single-output PID controllers for hemorrhage resuscitation and

IV propofol sedation. Note that these PID controllers preserved hemodynamic safety in all the 100 VPs when used individually. For realistic in silico evaluation, we considered sensor noise used in the design of the EKF as well as the limits on the fluid and propofol infusion doses (J_R and J_P ; according to the capacity of commercially available infusion pumps).

We conducted in silico evaluation of the proposed approach in a number of hemorrhage resuscitation-propofol sedation scenarios using diverse initial post-hemorrhagic BP-BIS states and therapeutic BP-BIS targets. To test the hypothesis that the proposed approach can enhance hemodynamic safety, we examined the boundedness of CO and TPR when the closed-loop hemorrhage resuscitation and IV sedation controllers were used in isolation vs in conjunction with the proposed approach. In addition, to test the hypothesis that the recursive therapeutic target guidance can retain the patients' therapeutic responses near the desired therapeutic trajectory, we examined the distribution of the final BP-BIS state pertaining to all the VPs in the presence vs absence of the recursive therapeutic target guidance.

V. RESULTS

Fig. 2 shows a representative example of the probabilistic reachability map in the BP-BIS space overlaid with the desired therapeutic target trajectory. Fig. 3 shows a representative example of BP-BIS (left) and CO-TPR (right) trajectories in the absence (upper panel) and presence (lower panel) of the proposed approach to reconcile the hemorrhage resuscitation and IV sedation control loops. Fig. 4 compares the final BP-BIS (left) and CO-TPR (right) states when (i) the control loops are not reconciled (upper panel); (ii) only the safetypreserving control but not the recursive target guidance component of the proposed approach is employed (middle panel); and (iii) the proposed approach is employed as a while (lower panel). Table I compares the distributions of BP and BIS errors as well as maximum CO and minimum TPR values in the absence and presence of the proposed algorithmic architecture for control loop reconciliation.

VI. DISCUSSION

The current progress in closed-loop control of critical care treatments reveals that an important prerequisite for deploying closed-loop controlled critical care to clinical practice is the assurance of hemodynamic safety endangered by potential conflicts between individual closed-loop controllers recruited in isolation with no account for control loop interference. This

work presented a novel reconciliation approach that can be readily employed with multiple individually designed single-input single-output closed-loop critical care controllers to assure hemodynamic safety in a patient and demonstrated its efficacy in hemorrhage resuscitation-IV sedation scenario.

The probabilistic reachability contour map was effective in visualizing the likelihood of reaching any therapeutic target as well as in deriving an adequate therapeutic trajectory. The representative example shown in Fig. 2 concerns a patient in a post-hemorrhagic state (BP 77 mmHg and BIS 93) that must be guided to a therapeutic target (BP 90 mmHg and BIS 60), whose reachability is estimated to be 50%. The recursive therapeutic target guidance directs patients along the derived therapeutic trajectory. The probabilistic reachability contour map may evolve into a stand-alone clinical decision-support system to guide the therapeutic target selection task.

The proposed approach was notably effective in preserving hemodynamic safety (Fig. 3 and Table I). For the scenario in Fig. 2, the proposed approach directed the VP only up to the intermediate target pertaining to the probabilistic reachability of 90% in Fig. 2 upon the violation of the R-CBF constraints (22) by the treatment inputs J_R and J_P computed by the isolated single-input single-output closed-loop controllers. All in all, the proposed approach preserved the boundedness in CO and TPR in 39 among the 50 hemodynamically unsafe VPs (50% of 100 VPs) in whom the boundedness constraints (18)-(19) were violated when closed-loop hemorrhage resuscitation and propofol sedation controllers were recruited in isolation. The approach judiciously pushed these VPs to patient-specific reachable intermediate targets while assuring hemodynamic safety via R-CBF-based control mediation, instead of blindly pushing them to the therapeutic target at the expense of unacceptably high CO and/or low TPR. All the 11 unsafe VPs were attributed to the parametric uncertainty,

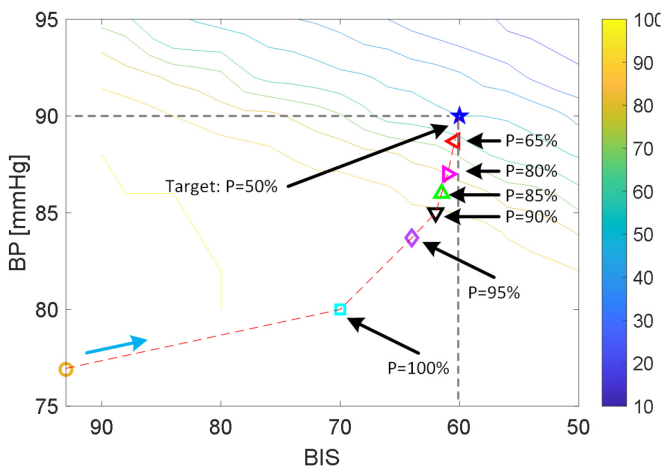


Fig. 2. Representative example of the probabilistic reachability contour map in the BP-BIS space, overlaid with the desired therapeutic target trajectory (dashed line) and intermediate therapeutic targets with decreasing reachability. The example concerns a patient in a post-hemorrhagic state (BP 77 mmHg and BIS 93) that must be guided to a therapeutic target (BP 90 mmHg and BIS 60), whose reachability is estimated to be 50%.

which led to inaccuracy in the EKF-based state estimation as well as the evaluation of the R-CBF inequality (22). In other words, the proposed approach assured the hemodynamic safety of all the VPs in the absence of parametric uncertainty in the EKF and R-CBF computations. However, the degree of excursions in CO and TPR outside of the admissible regime was small in all the VPs (lower panel in Fig. 4).

The recursive therapeutic target guidance was effective in retaining the therapeutic responses of the VPs in the vicinity of the desired therapeutic trajectory, especially compared to when it was not employed (compare middle vs lower panels in Fig. 4). Hence, recursive therapeutic target guidance may optimize the consistency in patient responses to treatments, thereby providing clinician users with enhanced predictability for the dynamic therapeutic response trajectory through time in all patients.

In sum, the evaluation results suggest that the proposed approach can be readily augmented with isolated hemorrhage resuscitation and IV propofol sedation controllers to reconcile therapeutic goals and hemodynamic safety via real-time state estimation, optimization-based control loop mediation, and recursive target guidance.

REFERENCES

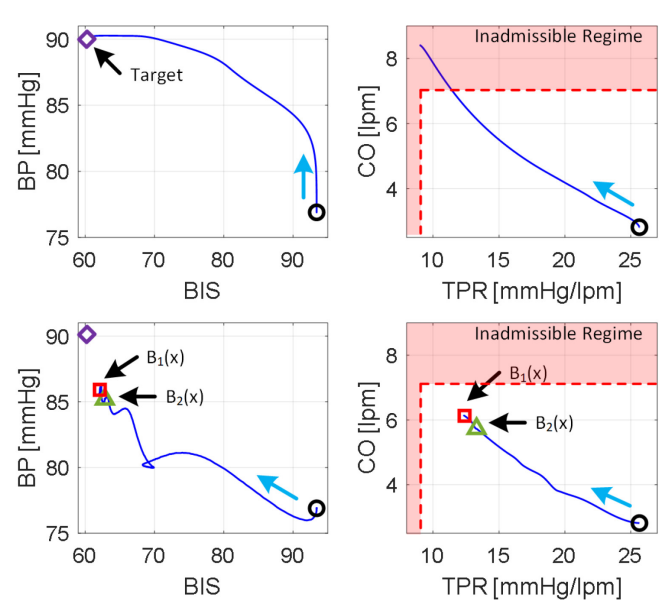


Fig. 3. Representative example of BP-BIS (left) and CO-TPR (right) trajectories in the absence (upper panel) and presence (lower panel) of the proposed approach to reconcile the hemorrhage resuscitation and IV sedation control loops. Red square and green triangle indicate the instants when the reciprocal CBFs $B_1(x)$ and $B_2(x)$ are in effect, respectively. Hemodynamic safety constraints are CO≤7 lpm and TPR≥9 mmHg/lpm. The proposed approach directed the VP only up to the intermediate target pertaining to the probabilistic reachability of 90% in Fig. 2 upon the violation of the reciprocal CBF constraints (22) by J_R and \check{J}_P computed by the isolated single-input singleoutput closed-loop controllers.

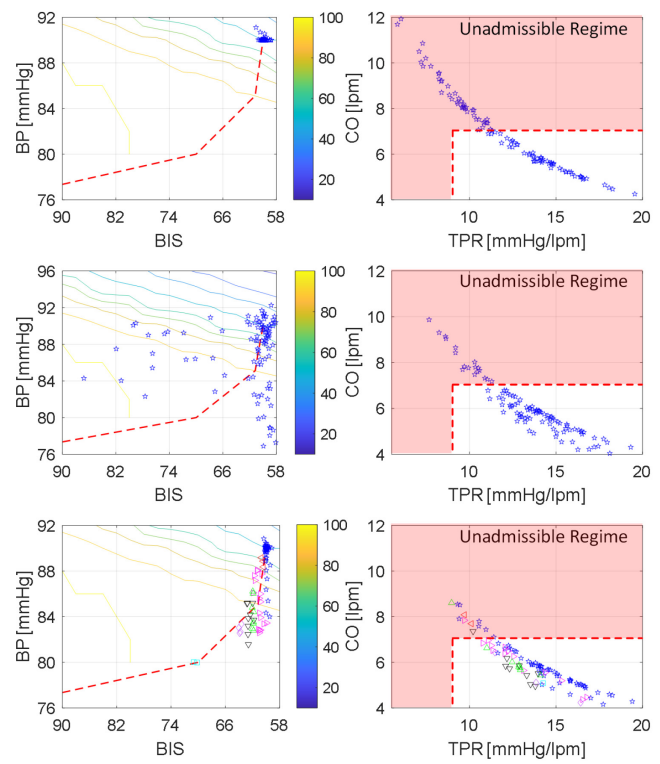


Fig. 4. Final BP-BIS (left) and CO-TPR (right) states when (i) the control loops are not reconciled (upper panel); (ii) only the safety-preserving control but not the recursive target guidance component of the proposed approach is employed (middle panel); and (iii) the proposed approach is employed as a whole (lower panel). Hemodynamic safety constraints are CO≤7 lpm and TPR≥9 mmHg/lpm.

- [1] B. Gholami, W. M. Haddad, J. M. Bailey, and W. W. Muir, "Closed-Loop Control for Fluid Resuscitation: Recent Advances and Future Challenges," Frontiers in Veterinary Science, vol. 8. Frontiers Media S.A., Feb. 23, 2021. doi: 10.3389/fvets.2021.642440.
- [2] B. L. Sng, H. S. Tan, and a. T. H. Sia, "Closed-Loop Double-Vasopressor Automated System vs Manual Bolus Vasopressor to Treat Hypotension during Spinal Anaesthesia for Caesarean Section: A Randomised Controlled Trial," *Anaesthesia*, vol. 69, pp. 37–45, 2014, doi: 10.1111/anae.12460.
- [3] A. Joosten et al., "Feasibility of Closed-Loop Titration of Norepinephrine Infusion in Patients Undergoing Moderate- and High-Risk Surgery," Br J Anaesth, vol. 123, no. 4, pp. 430–438, 2019, doi: 10.1016/j.bja.2019.04.064.
- [4] A. Joosten et al., "Feasibility of Fully Automated Hypnosis, Analgesia, and Fluid Management Using 2 Independent Closed-Loop Systems during Major Vascular Surgery: A Pilot Study," Anesth Analg, vol. 128, no. 6, pp. E88–E92, 2019, doi: 10.1213/ANE.000000000003433.
- [5] G. A. Dumont, "Closed-Loop Control of Anesthesia A Review," in IFAC Proceedings Volumes (IFAC-PapersOnline), 2012, vol. 45, no. 18, pp. 373–378. doi: 10.3182/20120829-3-HU-2029.00102.
- [6] J. Reinders, B. Hunnekens, F. Heck, T. Oomen, and N. van de Wouw, "Adaptive Control for Mechanical Ventilation for Improved Pressure Support," *IEEE Transactions on Control Systems Technology*, vol. 29, no. 1, pp. 180–193, Jan. 2021, doi: 10.1109/TCST.2020.2969381.
- [7] P. von Platen, A. Pomprapa, B. Lachmann, and S. Leonhardt, "The Dawn of Physiological Closed-Loop Ventilation - A Review," *Critical Care*, vol. 24. BioMed Central Ltd., p. Article Number 121, Mar. 29, 2020. doi: 10.1186/s13054-020-2810-1.
- [8] K. van Heusden et al., "Design and Clinical Evaluation of Robust PID Control of Propofol Anesthesia in Children," *IEEE Transactions on Control Systems Technology*, vol. 22, no. 2, pp. 491–501, 2014, doi: 10.1109/TCST.2013.2260543.

- [9] A. Joosten et al., "Automated Closed-Loop versus Manually Controlled Norepinephrine Infusion in Patients Undergoing Intermediate- to High-Risk Abdominal Surgery: A Randomised Controlled Trial," Br J Anaesth, vol. 126, no. 1, pp. 210–218, Jan. 2021, doi: 10.1016/j.bja.2020.08.051.
- [10]J. Rinehart, C. Lee, C. Canales, A. Kong, Z. Kain, and M. Cannesson, "Closed-Loop Fluid Administration Compared to Anesthesiologist Management for Hemodynamic Optimization and Resuscitation during Surgery: An In Vivo Study," *Anesth Analg*, vol. 117, no. 5, pp. 1119– 1129, 2013, doi: 10.1213/ANE.0b013e3182937d61.
- [11]A. Joosten et al., "Computer-Assisted Individualized Hemodynamic Management Reduces Intraoperative Hypotension in Intermediate- And High-risk Surgery: A Randomized Controlled Trial," Anesthesiology, pp. 258–272, 2021, doi: 10.1097/ALN.000000000003807.
- [12] A. Joosten et al., "Fully Automated Anesthesia and Fluid Management Using Multiple Physiologic Closed-Loop Systems in a Patient Undergoing High-Risk Surgery," A A Case Rep., vol. 7, no. 12, pp. 260– 265, Dec. 2016, doi: 10.1213/XAA.00000000000000405.
- [13]A. Joosten et al., "Feasibility of Fully Automated Hypnosis, Analgesia, and Fluid Management Using 2 Independent Closed-Loop Systems during Major Vascular Surgery: A Pilot Study," Anesth Analg, vol. 128, no. 6, pp. E88–E92, Jun. 2019, doi: 10.1213/ANE.0000000000003433.
- [14]A. Joosten et al., "Anesthetic Management using Multiple Closed-Loop Systems and Delayed Neurocognitive Recovery: A Randomized Controlled Trial," Anesthesiology, pp. 253–266, 2020, doi: 10.1097/ALN.00000000000003014.
- [15]A. D. Ames, X. Xu, J. W. Grizzle, and P. Tabuada, "Control Barrier Function Based Quadratic Programs for Safety Critical Systems," *IEEE Trans Automat Contr.*, vol. 62, no. 8, pp. 3861–3876, 2017, doi: 10.1109/TAC.2016.2638961.
- [16] W. Yin, A. Tivay, G. C. Kramer, R. Bighamian, and J. O. Hahn, "Conflicting Interactions in Multiple Closed-Loop Controlled Critical Care Treatments: A Hemorrhage Resuscitation-Intravenous Propofol Sedation Case Study," *Biomed Signal Process Control*, vol. 71, Jan. 2022, doi: 10.1016/j.bspc.2021.103268.
- [17]D. J. Eleveld, P. Colin, A. R. Absalom, and M. M. R. F. Struys, "Pharmacokinetic-Pharmacodynamic Model for Propofol for Broad Application in Anaesthesia and Sedation," *Br J Anaesth*, vol. 120, no. 5, pp. 942–959, 2018, doi: 10.1016/j.bja.2018.01.018.
- [18]H. Singh, "Bispectral Index (BIS) Monitoring during Propofol-Induced Sedation and Anaesthesia," Eur J Anaesthesiol, vol. 16, no. 1, pp. 31–36, 1999, doi: https://doi.org/10.1046/j.1365-2346.1999.00420.x.
- [19] A. D. Rafie et al., "Hypotensive Resuscitation of Multiple Hemorrhages using Crystalloid and Colloids," Shock, vol. 22, no. 3, pp. 262–269, 2004, doi: 10.1097/01.shk.0000135255.59817.8c.
- [20]F. de Wit et al., "The Effect of Propofol on Haemodynamics: Cardiac Output, Venous Return, Mean Systemic Filling Pressure, and Vascular Resistances," Br J Anaesth, vol. 116, no. 6, pp. 784–789, 2016, doi: 10.1093/bja/aew126.
- [21] A. Tivay, G. C. Kramer, and J.-O. Hahn, "Collective Variational Inference for Personalized and Generative Physiological Modeling: A Case Study on Hemorrhage Resuscitation," *IEEE Trans Biomed Eng*, vol. 69, no. 2, pp. 666–677, 2022, doi: 10.1109/TBME.2021.3103141.
- [22] D. M. Blei, A. Kucukelbir, and J. D. McAuliffe, "Variational Inference: A Review for Statisticians," *J Am Stat Assoc*, vol. 112, no. 518, pp. 859–877, 2017.
- [23]D. P. Kingma and M. Welling, "An Introduction to Variational Autoencoders," Foundations and Trends in Machine Learning, vol. 12, no. 4, pp. 307–392, 2019, doi: 10.1561/2200000056.
- [24]R. Ranganath, S. Gerrish, and D. M. Blei, "Black Box Variational Inference," *Journal of Machine Learning Research*, vol. 33, pp. 814–822, 2014.
- [25]M. D. Hoffman, D. M. Blei, C. Wang, and J. Paisley, "Stochastic Variational Inference," *Journal of Machine Learning Research*, vol. 14, pp. 1303–1347, 2013.
- [26] W. Yin, A. Tivay, and J.-O. Hahn, "Hemodynamic Monitoring via Model-Based Extended Kalman Filtering: Hemorrhage Resuscitation and Sedation Case Study," *IEEE Control Syst Lett*, vol. 6, pp. 2455–2460, 2022, doi: 10.1109/LCSYS.2022.3164965.
- [27] J. Valappil and C. Georgakis, "Systematic Estimation of State Noise Statistics for Extended Kalman Filters," AIChE Journal, vol. 46, no. 2, pp. 292–308, 2000, doi: 10.1002/aic.690460209.